https://doi.org/10.3311/PPci.21804

Periodica Polytechnica Civil Engineering, 67(3), pp. 925–935, 2023

Investigating the Effect of Low-Yield Yielding Dampers on the Seismic Behavior of Steel Frames

Kambiz Cheraghi[1*], Mohammad Hadi Tavana[2], Reza Aghayari[3]

[1] Department of Civil Engineering, Razi University, Kermanshah 6714414971, Iran
[2] Department of Civil Engineering, Kermanshah Branch, Islamic Azad University, Kermanshah 4121355671, Iran
[3] Department of Civil Engineering, Faculty of Engineering, Razi University, Kermanshah 6718997559, Iran
[*] Corresponding author, e-mail: kambiz.cheraghi@gmail.com

Received: 14 January 2023, Accepted: 07 May 2023, Published online: 17 May 2023

Abstract

Yielding dampers operate based on plastic deformations and energy dissipation. Given its low yield stress point and high ductility, low-yield steel is a suitable choice to build yielding dampers. In the present study, using the ABAQUS software, a number of pushover analyses have been carried out on a steel frame equipped with low-yield yielding dampers (LYDs). Therefore, using 40 pushover analyses, the effects of the number of the LYDs and the column's axial force have been evaluated. All of the models were analyzed and their force-displacement curves were obtained. Using the obtained, different seismic aspects of the frame – i.e., ductility, strength, energy dissipation, stiffness – were assessed. Also, to calculate the values of effective stiffness and yield and ultimate strengths, a number of analytical relationships have been formulated. Finally, contour plots have been obtained which can be used to calculate the stiffness of the proposed LYD. Comparing results showed that the damper can, to an acceptable level, improve the seismic parameters of the structure. Also, if the stiffness and yield strength of all of the LYDs added to the frame are, respectively, 3.25 and 0.13 times those of the bare frame, the frame will have its best performance.

Keywords

low-yield steel yielding dampers, steel moment resisting frame, ABAQUS, pushover analysis, finite element

1 Introduction

Yielding dampers are a class of passive damping devices capable of mitigating the seismic force applied to the structure by going through premature yielding. Up until this point, many studies have investigated the behavior of these dampers in different structures [1]. Introduced the vertical yielding shear link as an effective concept for the seismic rehabilitation of Reinforced Concrete (RC) structures and presented the necessary implementation criteria. The authors utilized the steel links that were attached to the beams of the structure, as yielding dampers and evaluated their behavior. The results indicated an improvement in the seismic behavior of the structure. In 2005, using experimental testing and numerical simulations, Shih and Sung [2] studied the hysteretic behavior of Added Damping And Stiffness (ADAS) dampers manufactured from Low Yield Steel (LYS) and A36 steel materials. The results showed that all of the models would have had high deformation capacities if LYS were used instead of A36. The behavior of central yielding dampers built from constructional and energy-absorbing steel materials in single-story steel frames with different opening percentages was investigate [3]. The results of this study indicated that if dampers made of energy-absorbing steel are used, it will improve the seismic of the frames and increase their energy dissipation capabilities. It was also shown that among all of the samples, the frame with 20% opening has the best performance [4]. Introduced a new yielding damper that can be used in the connections of steel structures. Through a series of theoretical and experimental analyses, the researchers demonstrated that the damper has a very suitable hysteretic behavior and can cause plastic hinge to occur in the damper itself.

In 2010, Maleki and Bagheri [5] Carried out an experimental and analytical study in yielding pipes and compared the performance of these elements in both hollow and concrete-filled conditions. The results of the study showed that due to a lack of ductility and the crushing of the concrete (as a result shear loading), the concrete-filled

Cite this article as: Cheraghi, K., Tavana, M. H., Aghayari, R. "Investigating the Effect of Low-Yield Yielding Dampers on the Seismic Behavior of Steel Frames", Periodica Polytechnica Civil Engineering, 67(3), pp. 925–935, 2023. https://doi.org/10.3311/PPci.21804

pipes undergo failure. Despite this, the pipe itself remains intact, causing further energy dissipation in the structure [6] introduced a type of grooved damper. Through a series of tests on a number of experimental samples, the authors concluded that increasing the widths of the grooves would increase the energy dissipation capacities and shear force of the samples. Also, theoretical relationships whose results were quite close to experimental results were also introduced to calculate the parameters of the damper. The dampers are also employed to reduce the dynamic response of the structure to seismic loading [7–10]. Seismic energy-absorbing systems are used in structures in the form of metallic yielding dampers, friction dampers [11–13], and viscoelastic dampers [14].

Ebadi Jamkhaneh et al. [15], proposed a cylindrical damper which could be used as a yielding element in structures. Using a number of experimental models and numerical simulations in ABAQUS, the authors demonstrated that the models respond suitably to cyclic loads. Experimental and numerical investigations carried out by [16, 17] have demonstrated that ADAS and Triangular Added Damping and Stiffness (TADAS) dampers improve the structure's behavior. The results of these investigations showed that when the yield shear force of these dampers and the base shear of the frame are equal, the frame will have its best structural performance. Other yielding elements have also been introduced (e.g., Bar damper [18, 19] which are used to absorb a portion of the seismic energy.

Yao et al. [20] in 2021 performed experimental and numerical evaluations on low-yield-point steel shear panel dampers. The study utilizes square steel tube stiffeners for the core plates, which were also made from low-yield-point steel with low yield stress. The results show that square steel tubes are very efficient in preventing the core plates against out-of-plane deformations.

The general rule is that yielding dampers should yield prior to the structure's main components. This mechanism will absorb the energy entering the structure; therefore, the number of yielding components used in the structure is very important. If too few dampers are used, the improvement might be insignificant. Conversely, if too high a number of yielding plate are employed, they might yield after the structure's main components. Because of its lower yield point and high ductility, low-yield steel is a suitable material choice to manufacture these elements. In the present work, first, a single-bay single-story steel frame was modeled using the ABAQUS finite element software. Then, the steel frame was equipped with Low-yield Yielding dampers (LYDs) with reduced geometries. The plates were attached to the frame using a Chevron brace. Through 40 pushover analyses, the effects of the number of LYD and the column's axial load on the different parameters of the frame – i.e., stiffness, ductility, energy dissipation, and strength – have been probed. The number of LYDs varies from 1 to 9. Also, the axial force was applied to the column in four different magnitudes. These were equal to 0%, 15%, 30%, and 45% of the columns' critical load.

When lateral load is applied to the frame, it is divided proportional to the stiffnesses of the dampers and the frame. As mentioned before, these dampers have to be designed so that they yield prior to the other components of the structure. This means that calculating the stiffness and strength of these elements is very important. For this reason, analytical relationships have been formulated to calculate the values of yield and ultimate strengths and stiffness of the dampers. The values produced by these relationships are very close to those obtained from the numerical analyses. Furthermore, to calculate the stiffness of the proposed plates with different dimensions, a series of contour plots have been presented which can be used to acquire a quicker estimation of the plates' stiffnesses. These plots are also very useful in the design of these types of dampers. The results of the numerical analyses have revealed that LYDs can improve the seismic parameters of the frame in which they are used to an acceptable degree. Also, if an appropriate number of LYDs are used, they can minimize the effect of axial force on the ductility of the frame.

2 Verification of the numerical models

2.1 Verification of steel frame

To verify the numerical model, the single-story single-bay steel frame tested by [21] has been used. The experimental model and its details are shown in Fig. 1.

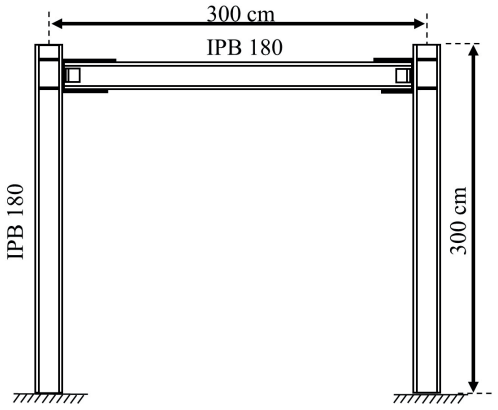

Fig. 1 The experimental steel frame and its details [21]

The experimental sample has been modeled using 8-node solid elements (C3D8R) in ABAQUS. Since no failure was seen in the welds during loading, all of the connections of the sample were modeled using the "Tie" constraint. This constraint means that no independent movement occurs between the two members. When two elements of the structure are completely welded together, it can simulate the behavior of the model properly. Also, the analysis was carried out using a quasi-static approach and the Newton-Raphson method. Finally, the columns' connection to the lab's floor was modeled using a fixed connection, given that no failure was seen during the test.

Based on the results of a mesh sensitivity analysis, a size of 3 cm was determined to discretize the numerical model. The discretized model at the end of loading is shown in Fig. 2. After the analysis, the backbone diagram was obtained and compared to the numerical results (Fig. 3). It can be seen that the obtained results are in very good agreement, meaning that the numerical model is reliable enough to be used for further analyses.

2.2 Verification of LYD

In order to verify the numerical LYD, single LYD plate (Fig. 4(a)) was modeled in ABAQUS using shell element. It can be seen that the dimensions of LYD are *h*, *b*, *r*, *t*, which represent the thickness of the LYD, the opening radius of the half circle on each sides, and the width and the height of the LYD. Then it was analyzed by non-linear static analysis. Boundary conditions of the LYD in ABAQUS shown in the Fig. 4(b). After the analysis, the diagram of its force-displacement was extracted from ABAQUS, which is demonstrate in Fig. 4(d). in this figure, the stiffness and yield strength of the plate are also shown.

In order to verify the ABAQUS result, the stiffness and yielding parameters of this plate were compared with the theoretical relations, which are presented below.

In the following, a series of analytical relationships have been formulated to compute the stiffness and yield strength of the proposed yielding plate. When the LYDs is completely welded to the upper and lower plates, rotation on both ends of the plates is roughly equal to zero, which means that they can be considered as guided supports. This type of member stiffness can be determined using the Castigliano's method [22] (Fig. 4(b)). When bending and shear forces influence displacement, the formation of this

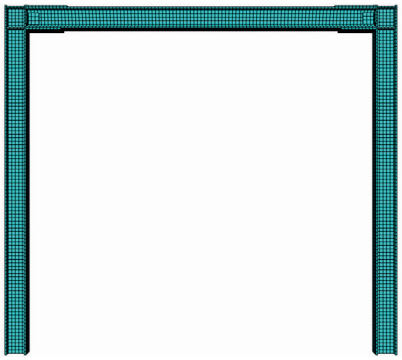

(a)

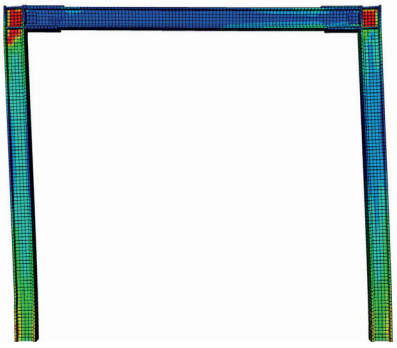

(b)

Fig. 2 (a) FEM model, (b) The model deformation after loading

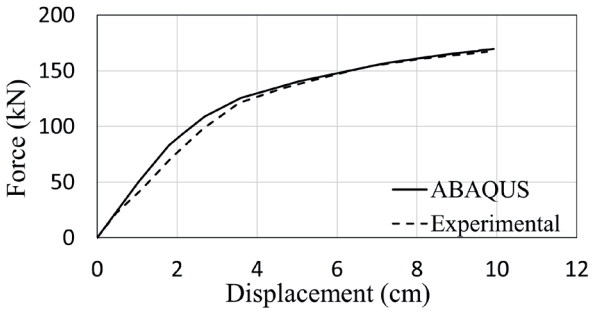

Fig. 3 Comparison of the experimental and numerical force-displacement curves

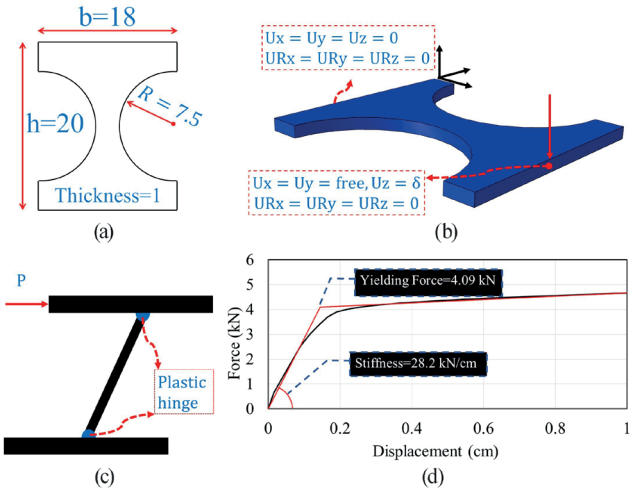

Fig. 4 (a) Dimensions of the LYD, (b) Boundary condition of yielding plate, (c) Mechanism of the yielding plate, (d) Force-displacement curve and its equivalent bilinear

method is in the form of Eq. (1). Based on this formula, the stiffness of the proposed plate can be calculated via Eq. (3), which yields the value of 28.57 kN/cm and is close to the numerical results calculated in Fig. 4(d) (28.2 kN/cm).

$$U_z = \int_0^L \frac{M \partial M / \partial p}{EI} dx + \int_0^L \frac{V \partial V / \partial p}{5/6\, GA} dx \tag{1}$$

$$b(x) = 2(9 - \sqrt{7.5^2 - (x-10)^2})$$

$$U_z = \int_0^{2.5} \frac{P(x-10)^2 \times dx}{2\times10^4 \frac{18\times1^3}{12}} + \int_0^{2.5} \frac{P \times dx}{0.32\times2\times10^4\times18\times1}$$

$$+\int_{2.5}^{17.5} \frac{P(x-10)^2 \times dx}{2\times10^4 \frac{b(x)\times1^3}{12}} + \int_{2.5}^{17.5} \frac{P \times dx}{0.32\times2\times10^4\times(18-b(x))\times1}$$

$$+\int_{17.5}^{20} \frac{P(x-10)^2 \times dx}{2\times10^4 \frac{18\times1^3}{12}} + \int_{17.5}^{20} \frac{P \times dx}{0.32\times2\times10^4\times18\times1} = \delta \tag{2}$$

$$U_z = 0.035P = \delta \rightarrow k = \frac{p}{\delta} \rightarrow k = 28.57 KN/cm \tag{3}$$

After increase in the p value due to the presence of maximum moment in the support, plastic hinges start to form in these areas (Fig. 4(c)). The force causing the creation of plastic hinges in both ends of the plate is equal to the plate's yield strength, which can be calculated via Eq. (4).

$$V_{e_d} = \frac{b \times t^2}{2h} \sigma_{y_{(LYS)}} \tag{4}$$

In Eq. (4), the parameters b, t, h are the width, thickness, and height of the LYDs, respectively. Also, $\sigma_{y_{(LYS)}}$ represent the yield stresses of the LYD, which, according to Fig. 7, are equal to 100 Mpa. By substituting the dimensions of the LYD shown in Fig. 4(a) in Eq. (4), the yield strength is equal to 4.5 kN, that is close to the numerical results 4.09 kN calculated in Fig. 4(d).

3 The main models

To evaluate the influence of the LYDs, the verified frame (with the same dimensions and properties) was equipped with the proposed LYDs (Fig. 5). The LYDs was attached to the beam using a Chevron brace (Fig. 5). The frame's braces were designed so that they do not buckle when the maximum number of LYDs are installed on the frame.

The variables of the frame include the number of LYDs and the columns' axials force, with the former ranging from 1 to 9 and the latter taking on the values of 0%, 15%, 30%, and 45% of the columns' critical load. In accordance with the AISC standard [23], the critical load of the column was computed to be equal to 1028 kN. The numerical analyses were carried out in two stages: in the first step, the columns' axial forces were applied, and in the second step, lateral load was applied to the top of the frame.

The following assumptions have been made in the numerical model:

- Due to their low thickness, the LYDs were modeled using the S4R shell element [24].
- All of the components of the model were connected to one another using the "Tie" command of ABAQUS. Also, for both ends of the yielding dampers, the shell-to-solid-coupling tie was used.
- The numerical analysis in ABAQUS was performed using the quasi-static approach and the Newton-Raphson method.
- Based on the carried-out mesh sensitivity analysis, the mesh size of the LYDs and the other members were considered equal to 1 cm and 3 cm, respectively.

The discretized model of the frame equipped with the proposed yielding plate is shown in Fig. 6.

Specifications of the low-yield steel used to build the LYDs were taken from the study carried out by [25]. Also, the material specifications of the other components of the frame (ST 37 steel) [26], assumed in the numerical model are illustrated in Fig. 7.

To make the interpretation of the results more convenient, the terminology given in Table 1 has been used to label the main models. As it can be seen, the models have been labeled based on the number of LYDs and the columns' axial forces. For instance, the name "M7-15" represents a model that has 7 LYD (for example Fig. 6) and an axial force equal to 15% of the column's critical load. (It should be noted that the complete specification of model sections are shown in Fig. 5)

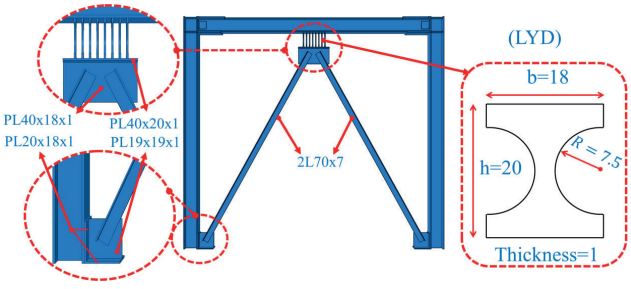

Fig. 5 Section properties of the main model and dimensions of the LYD (cm)

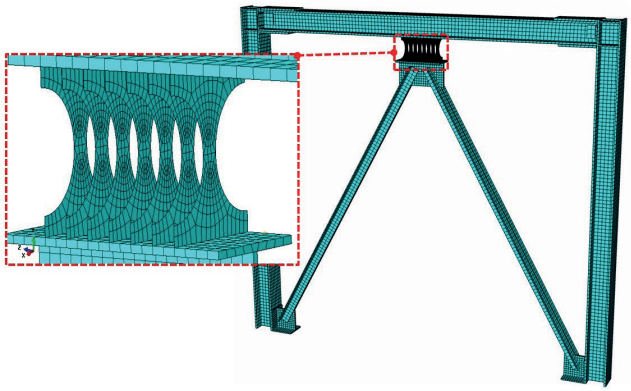

Fig. 6 Meshed model equipped with LYD

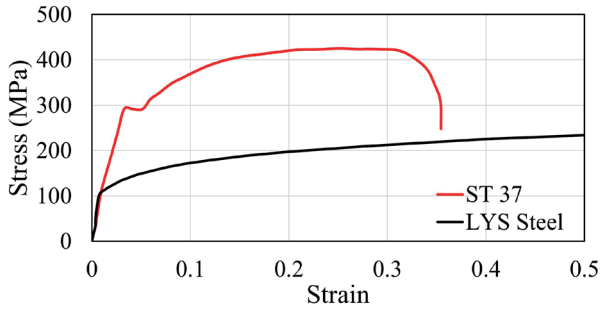

Fig. 7 Properties of the LYDs and ST 37 (beam, columns, brace, and the connecting plates) steel materials [25, 26]

The following considerations are important in the design of the LYDs:

- If the number of the LYDs is low, their full capacities will not be utilized. By contrast, if the number is high, the dampers will yield after the structure's main components, which is not a desired outcome.
- These dampers have to be installed in a place where they can absorb the maximum deformation when the frame is subjected to lateral drift.
- These dampers also increase the strength and stiffness of the structure.
- The structure's braces have to be designed so that they do not buckle prior to the full yielding of the yielding plates.

Therefore, there is a specific number of LYDs in the presence of which the frame will have its best structural performance. One of the main objectives of the present study is to find this suitable number.

4 Bilinearization of the force-displacement curve and the numerical results

The According to the FEMA 440 [27] guideline, the force-displacement curve can be approximated by a simplified bilinear diagram (Fig. 8). Using this simplified bilinear

Table 1 The models

Name	No. of LYDs	Axial load
M0-0, M0-15, M0-30, M0-45	w/o damper	0 Pcr, 0.15 Pcr, 0.3 Pcr, 0.45 Pcr
M1-0, M2-0, … , M9-0	1, 2, … ,9	0 Pcr
M1-15, M2-15, … , M9-15	1, 2, … ,9	0.15 Pcr
M1-30, M2-30, … , M9-30	1, 2, … ,9	0.3 Pcr
M1-45, M2-45, … , M9-45	1, 2, … ,9	0.45 Pcr

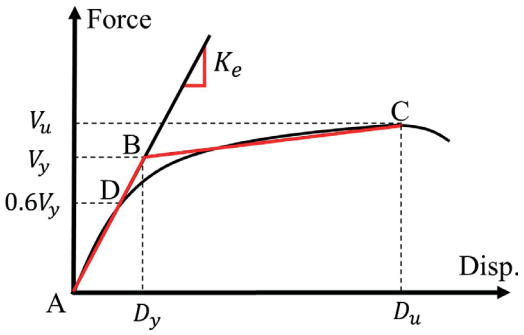

Fig. 8 Simplified force-displacement curve

model, the lateral effective stiffness (K_e) and the effective yield shear (V_y) can be calculated. To simplify the nonlinear behavior, point B has to be selected so that the area underneath the bilinear diagram be equal to the area underneath the nonlinear curve. Furthermore, the length of the AD line has to be equal to 0.6 AB. This way the, the force corresponding to point B would be equal to V_y, and for a base shear of $V_y \times 0.6$ in the nonlinear curve, the secant modulus would represent the lateral effective stiffness (K_e). In the simplified model, one should be wary that V_y not be greater than the maximum base shear in the nonlinear curve.

$$K_e = \frac{V_y}{D_y} \tag{5}$$

$$Ductility = \frac{D_u}{D_y} \tag{6}$$

Eqs. (5) and (6) describe effective stiffness and ductility, respectively. Also, the ultimate strength of the frame is equal to V_u in Fig. 8. Finally, the area enveloped under the curve represents the model's energy dissipation capacity. These four parameters have been calculated and compared for the main models. In Fig. 9, four force-displacement curves and their corresponding equivalent bilinear diagrams are shown which correspond to models M6-0, M2-15, M5-45, and the bare frame (no column axial force). A drift of 4% was applied to the each of the main models. In this figure, the blue curve is the results of ABAQUS and the red one is the equivalent bilinear.

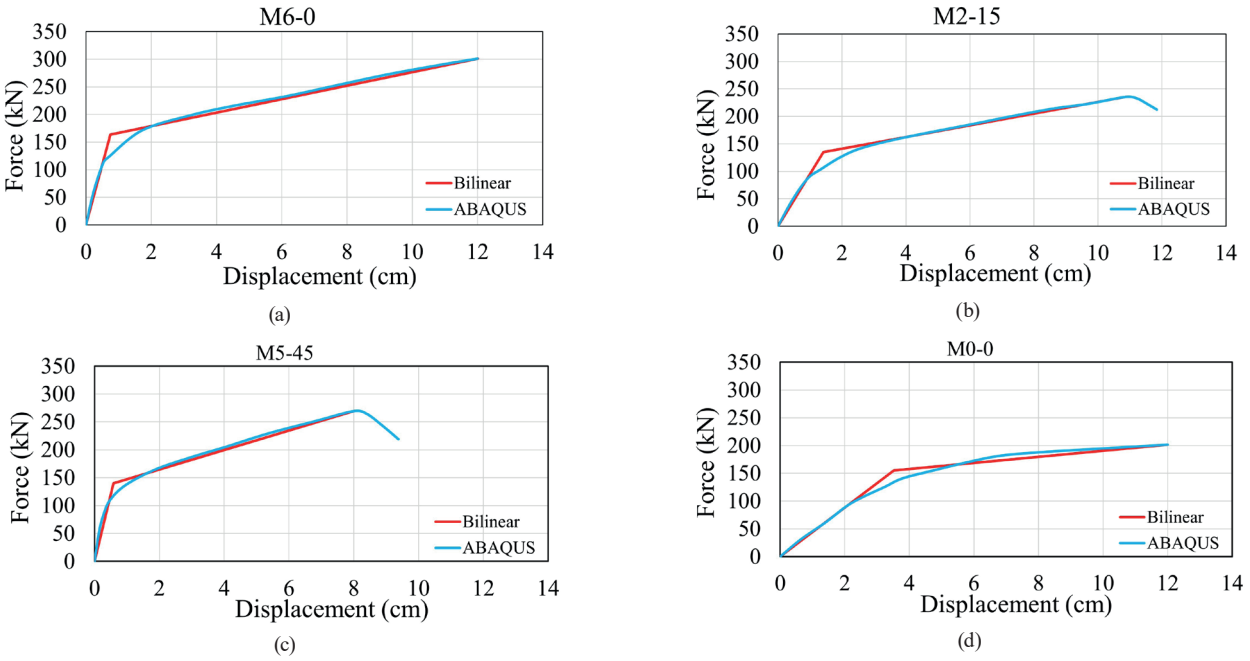

Fig. 9 Nonlinear and equivalent bilinear curves corresponding to models: (a) M6-0, (b) M2-15, (c) M5-45, (d) M0-0

Fig. 10(a) illustrates the Von Mises stress contours of the LYDs. It can be seen that large areas of both ends of the yielding plates have gone through yielding. Due to the minimum value of bending moment happening in the medial zone of the plate (along the height), this area has yielded after all of the other parts of the yielding plate. Also, the plate's rotation about the X axis has been shown in Fig. 10(b). It can be seen that both ends have slopes of approximately zero, with the maximum value being in the reduced zone of the LYD.

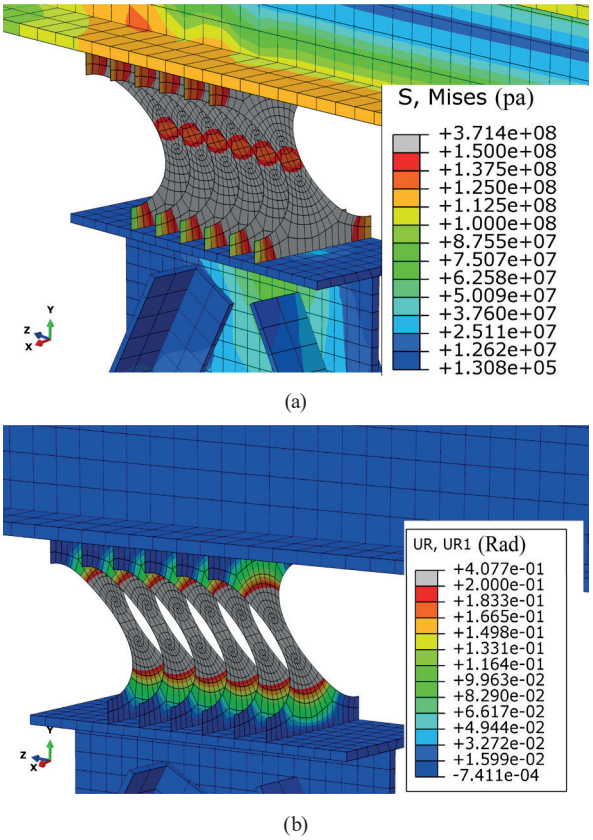

Fig. 10 (a) Von Mises and (b) Rotation about the X Axis contours of LYDs (M6-0)

4.1 Assessing the ductility and energy dissipation of the models

In this section, the effects of axial load and number of LYDs on the ductility and energy dissipation of the steel frame will be evaluated. Fig. 11(a) presents the energy dissipation of the models. As the columns' axial forces increase, the models also experience a decline in their energy dissipation capacities, with the effect being most noticeable when axial load is equal to 15% of the column's critical load. Increasing the number of LYDs to 6 increases the energy dissipation of all of the models. However, adding more LYD causes a decline in the curve. When 6 plates are used in the frame, the energy dissipation of the frame enhance by an average of 56% when compared to the frame with no dampers, an indication of the suitable efficiency of this type of damper. Also, for each 15% increment in the columns' axial loads, the frame experienced a 13% decline in its energy dissipation.

Fig. 11(b) presents the ductility of the models. As seen, increase in the columns' axial loads leads to a decrease in the frame's ductility. When the number of LYDs is equal to 5, increase in the axial load causes its least strength

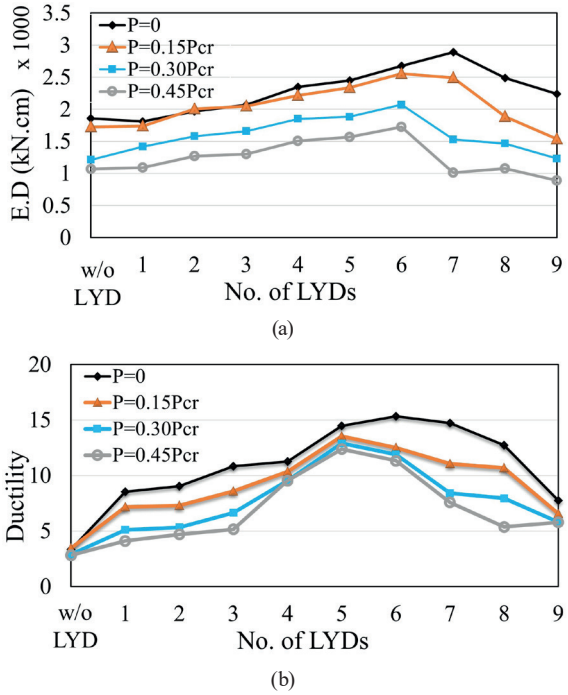

Fig. 11 Effects of the number of LYDs and column axial load on (a) Energy dissipation and (b) Ductility coefficient

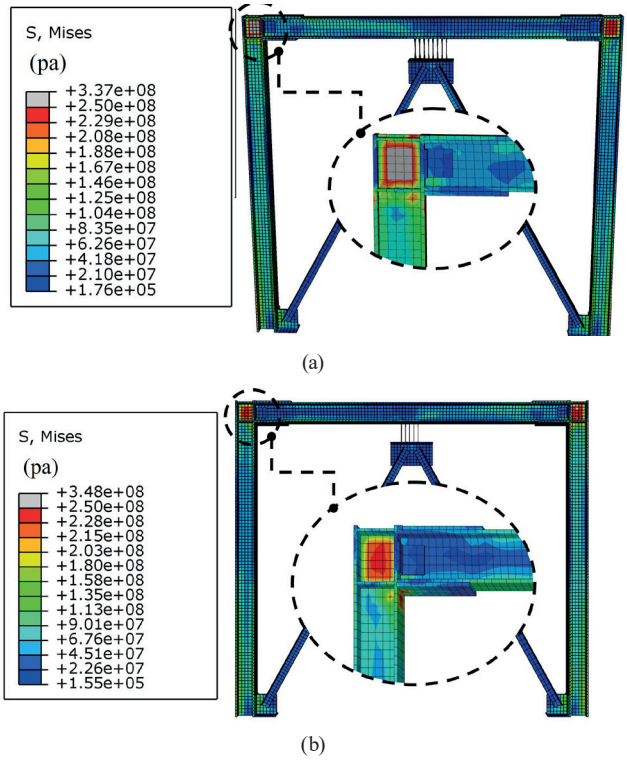

Fig. 12 Von-Mises stress in lateral displacement of 2.2 cm (a) M8-0 (at beginning of yielding) (b) M5-0

degradation. This shows that when an appropriate number of LYDs are used, the influence of column axial load in decreasing the ductility of the frame can be minimized.

When the number of LYD is exceeded 6, due to the high strength of the LYDs, the frame will yield in less drift. The Fig. 12 shows the stress contour of M5 and M8 models. The frames shown in Fig. 12, are in the lateral displacement of 2.2 cm. At this moment, the first part has been made in the frame with 8 LYDs, but no part of the frame has been yielding yet. In the frame with 5 LYDs, the first part of yielding occurred at 3 cm lateral displacement. In this regard, if the number of LYDs is high, it will cause the main members of the frame to yield sooner which is considered a negative aspect.

4.2 Analytical relationships to calculate the stiffness and strength of the plates

When lateral load is applied to the frame, it is doled out among the load-bearing elements based on their stiffnesses. Also, the damping elements have to be designed so that they yield prior to the main components of the frame, which is why the calculation of the stiffness and strength of these plates is very important. As shown in Section 2.2, formulas were presented to calculate the stiffness (Eq. (1)) and yield strength (Eq. (4)) of the LYD. In this section, these two parameters were calculated for different dimensions of the sheet and compared with the results of ABAQUS.

After the yielding of both ends of the plate as a result of strain hardening, will have a higher force carrying capacity. The maximum force that can be borne by the plate can be computed using Eq. (7).

$$V_{u_d} = \frac{bt^2}{2h}\sigma_{u_{(LYS)}} \tag{7}$$

In Eq. (7), the parameters $\sigma_{u_{(LYS)}}$ represent the yield and ultimate stresses of the LYD, which, according to Fig. 7, are equal to 100 Mpa.

To compare the results obtained from Eqs. (1) and (4), additional numerical analyses were performed on the yielding plate. Fig. 13(b) shows the loading and support conditions of the numerical models. Given that the aim is to calculate the values of stiffness yield strength of the plate, the analysis continued until a displacement of 1 cm along the Z direction. Fig. 12(a) depicts the stress contour of the models after loading.

To compare the stiffnesses of the plates, the radius R (It was introduced in Section 4.2) was considered as a variable and 9 numerical analyses were carried out on the plate. Then, the stiffness of the plate was obtained from the force-displacement curve. Finally, the results were compared to those calculated using Eq. (1) (Fig. 14). It can be seen that the results have very good agreement.

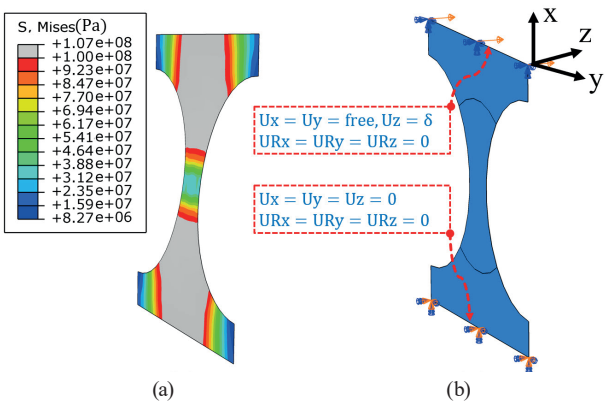

Fig. 13 (a) Stress contour after loading, (b) Support conditions of the yielding plate in Fig. 4(a) dimension

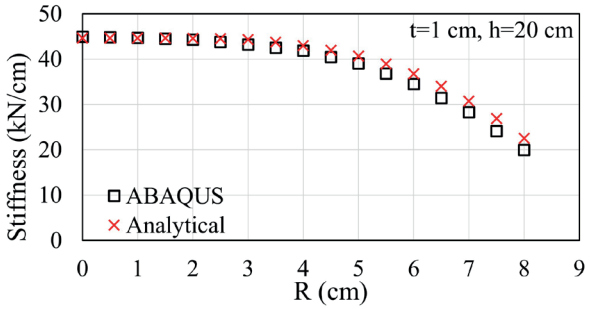

Fig. 14 Comparison of the stiffness of LYD obtained from ABAQUS and Eq. (1)

Five numerical analyses were carried out on the yielding plate to compare the results to those obtained from this equation. It should be mentioned that the only variable in these analyses was the thickness of the plate. Then, the force displacement curves of the plate and their corresponding equivalent bilinear diagrams were derived (Fig. 15(a)). The comparison of the yield strength values obtained from numerical simulations and Eq. (6) is shown in Fig. 15(b). A very good agreement can be seen between the numerical and analytical results, which means that by using the proposed equation, a reliable result can be reach much quicker.

4.3 Assessing the strengths and stiffnesses of the models

This section investigates the effects of the number of LYDs and the column's axial load on the stiffness and strength of the steel frame (shown in Fig. 5). Fig. 16(a) shows how to number of LYDs influences the frame's stiffness. It can be seen that an increase in the number of LYDs and axial force results in an increase in stiffness. On average, each 15% increase in the column's axial force brings about a 19 kN/cm increase in stiffness. Also, adding one LYD increases the overall stiffness of the frame by 26.2 kN/cm, a number that differs from the value produced by Eq. (4) – i.e., 28.57 kN – by a small amount.

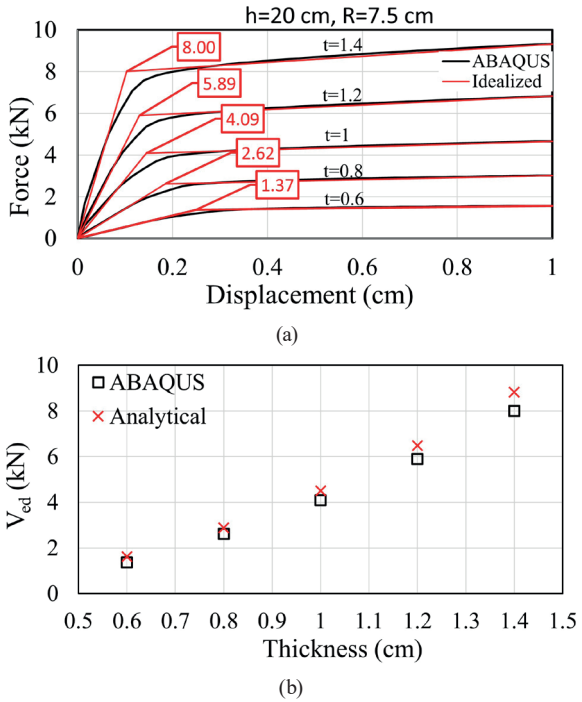

Fig. 15 (a) Force-displacement and bilinear curve of LYD in ABAQUS, (b) Yield strength comparison from ABAQUS and Eq. (4) (Fig. 4(a) dimensions)

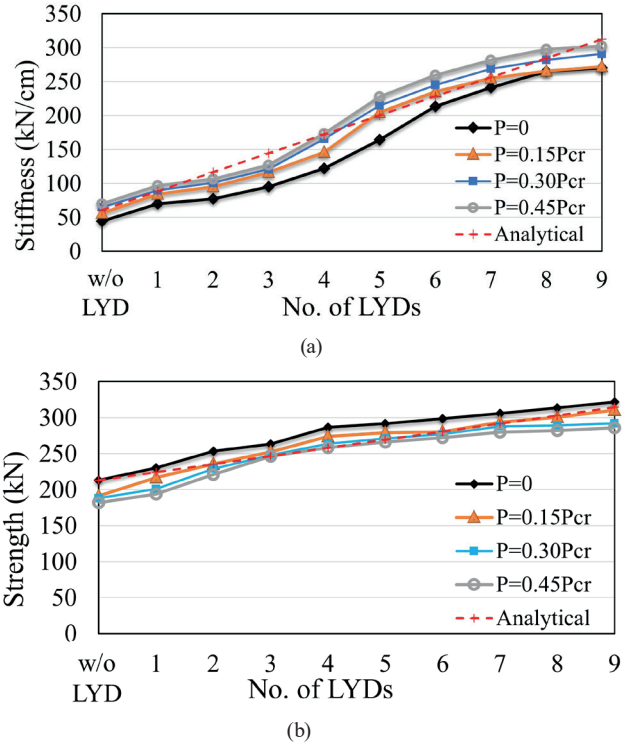

Fig. 16 Effect of the number of LYDs on (a) Effective stiffness, (b) Ultimate strength of the steel frame (Fig. 5)

Fig. 16(b) displays the strengths of the samples with respect to the number of LYDs and column axial force. It can be seen that as a result of adding the plates, the frame

has experienced a somewhat linear strength increase. Adding a single LYD to the frame has increased its strength by an average of 11.1 kN, which is quite close to 11.25 kN, the value yielded from Eq. (7). Furthermore, the columns' axial force has reduced the frames ultimate strength in all conditions, with each 15% increment causing an average of 15.5 kN decrease in the frame's strength.

4.4 Calculating the stiffness of the yielding plate for different sizes

Since in the design of the structure, the two parameters of yield strength and effective stiffness of the LYDs are very important, six contour plots have been shown in Fig. 17 to quickly calculate the stiffness of the proposed LYD. The yield and ultimate strengths of the plates can be conveniently calculated using the Eqs. (6) and (7), respectively. Therefore, only the contour plots that can be used to calculate stiffness have been presented. The stiffness of a LYD with the specifications shown in Fig. 4, a thickness t, and when its height and width are the same ($h = b$), if can be calculated using Eq. (3). The results generated by this equation are shown in the curves given in Fig. 17. These curves have been obtained for values of b ranging from 16 cm to 24 cm. In these curves, the horizontal and vertical axes represent, respectively, radius (R) and thickness of the plate, in which h is equal to b and have constant values.

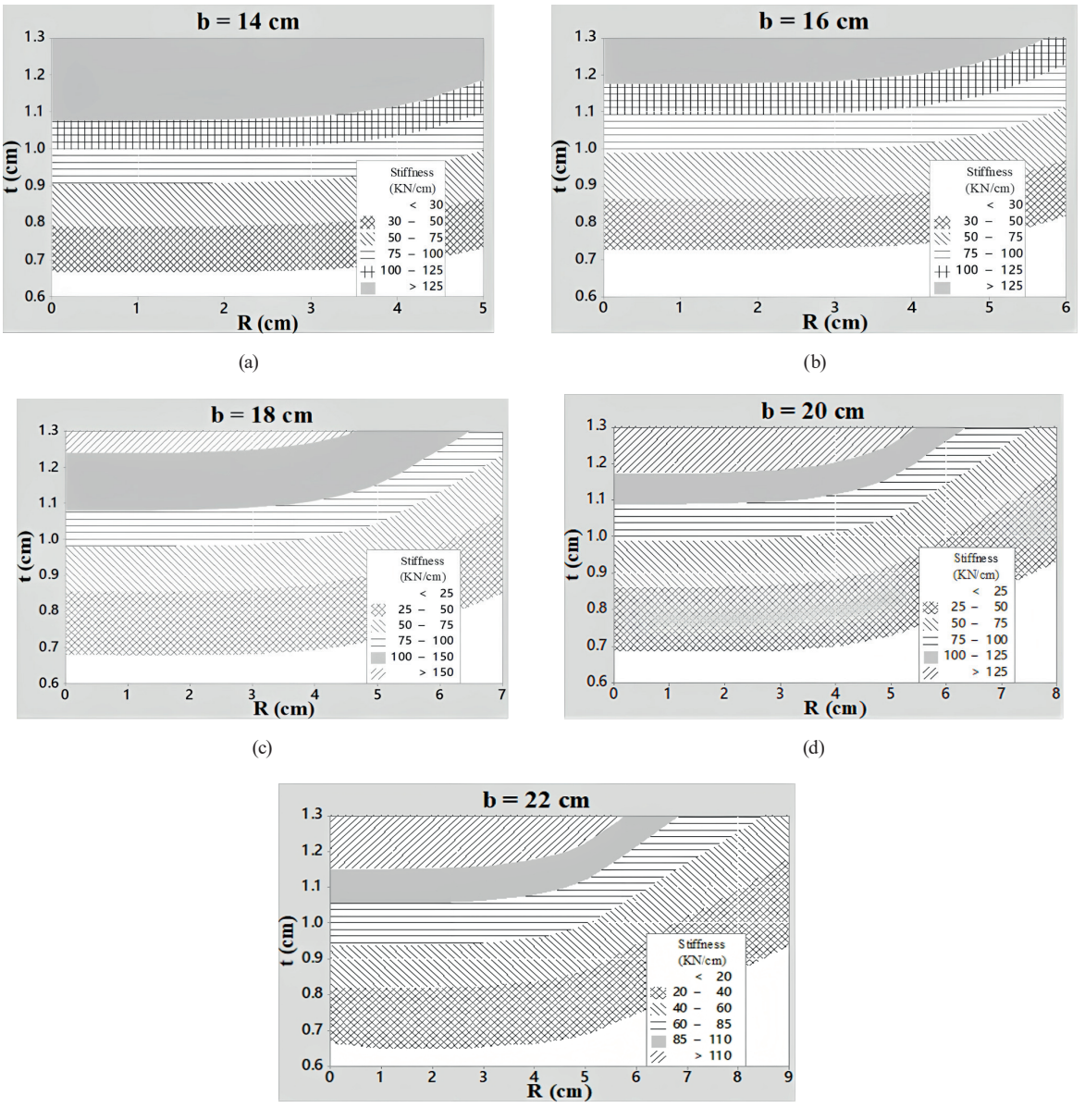

Fig. 17 Stiffness of the LYD (Fig. 4(a)) obtained using Eq. (1) (a) $h = b = 14$, (b) $h = b = 16$, (c) $h = b = 18$, (d) $h = b = 20$, (e) $h = b = 22$

To calculate the stiffness, due to the complexity of the calculation of the Eq. (3), a formula was introduced in the form curve fitting, which can be achieved by good accuracy to the results of the 3 formulae. In Table 2, the results of the analytical Eq. (1) and the approximate Eq. (8) was compared. It should be noted that all the units are used in the Eq. (8) must be in kN and cm.

$$K_e = t\sqrt{b} - 0.036b + \frac{14315.2t^{2.97}e^{-0.046R}}{b^{1.865}} \quad (8)$$

Table 2 Comparison of Eqs. (3) and (8) results to calculate stiffness

Dimensions of the LYD (cm)			Stiffness (kN/cm)		Err. (%)
b	*R*	*t*	Eq. (1)	Approximate Eq. (8)	
14	0	1.1	133.25	137.92	3.4
14	4	1.1	119.65	116.85	2.4
16	1	0.6	16.8	17.06	1.52
16	5	1.3	143.3	143.14	0.11
18	0	0.7	21.07	21.98	4.14
18	5	0.7	19.25	19	1.85
20	1	0.6	10.77	11.1	3.06
20	7	1.3	83.55	87.43	4.44
22	0	0.6	8.9	9.05	1.66
22	8	0.9	22.09	24.48	9.76
24	1	0.8	17.72	18.72	5.34
24	7	0.6	6.7	6.8	1.33

5 Conclusions

In this study, steel frames equipped with LYDs have been evaluated using pushover analyses in ABAQUS. First, and experimental single-story single-bay steel frame was verified using ABAQUS. furthermore, to ensure the accuracy of LYD results in ABAQUS, its stiffness and yield strength parameters were compared with theoretical formulas. Then, yielding plates made of low-yield steel were installed on the frame. Forty numerical analyses were carried out to evaluate the seismic performance of the frame. The effects of two variables – namely, the number of the LYDs and the column's axial force – were assessed on the results of the numerical simulations. After carrying out the pushover analyses, the nonlinear curves and their corresponding equivalent bilinear diagrams were derived. Afterwards, the seismic parameters of the steel frame – i.e., stiffness, strength, ductility, and energy dissipation – were calculated for all of the models.

Analytical relationships were proposed to calculate the stiffness, and yield and ultimate strengths of the yielding plates, and the results were compared to those obtained from numerical analyses. Finally, for a quicker calculation of the stiffness of the proposed yielding plate with different dimensions, contour plots were presented. From these, using the radius of the openings and the plate's thickness, the value of the stiffness can readily be obtained with acceptable accuracy. The conclusions of this study are as follows:

- The axial force of the column causes a considerable decrease in the ductility of the steel frame. However, using an appropriate number of LYDs (for the frame studied herein, this number is equal to five) minimizes this decrease.
- Increasing the number of LYDs to six would increase the frame's energy dissipation. However, higher numbers would have the opposite effect. For compatibility with the ductility results, it is recommended to use five yielding dampers. In this way, the frame would have an energy dissipation capacity 42% greater than that of the bare frame.
- Increase in the column's axial force reduces the strength and stiffness of the steel frame. As a result of each 15% axial force increment, the frames strength and stiffness undergo reductions of 4% and 10%, respectively.
- The formulae presented to calculate the stiffness and yield and ultimate strengths of the LYD produced results that are in very good agreement with the results of the numerical analyses. The opening radius (R) of the proposed yielding plate does not exert any influence on the yield and ultimate strengths of the plate; it does, however, affect the plate's stiffness. Also, using the diagrams shown in Fig. 17, the stiffness of the yielding plate can be estimated quite quickly, which is something very useful in the design of structures equipped with this type of yielding plate.
- A formula was proposed that can calculated the stiffness of the yielding plate using the damper parameters that can be very useful for designing this damper in the structure.
- It is recommended for the stiffness and collective strength of the LYD added to the frame to be 3.25 and 0.13 times those of the initial steel frame. This way, it can be ensured that the ductility coefficient and energy dissipation are maximized, and that the column's axial force will have the smallest possible influence on the results.

References

[1] Ghobarah, A., Abou Elfath, H. "Rehabilitation of a reinforced concrete frame using eccentric steel bracing", Engineering Structures, 23(7), pp. 745–755, 2001. https://doi.org/10.1016/S0141-0296(00)00100-0

[2] Shih, M.-H., Sung, W.-P. "A model for hysteretic behavior of rhombic low yield strength steel added damping and stiffness", Computers & Structures, 83(12–13), pp. 895–908, 2005. https://doi.org/10.1016/j.compstruc.2004.11.012

[3] Sabouri-Ghomi, S., Roufegarinejad, A. "Non-linear behavior of yielding damped braced frames", The Structural Design of Tall and Special Buildings, 14(1), pp. 37–45, 2005. https://doi.org/10.1002/tal.257

[4] Oh, S.-H., Kim, Y.-J., Ryu, H.-S. "Seismic performance of steel structures with slit dampers", Engineering Structures, 31(9), pp. 1997–2008, 2009. https://doi.org/10.1016/j.engstruct.2009.03.003

[5] Maleki, S., Bagheri, S. "Pipe damper, Part I: Experimental and analytical study", Journal of Constructional Steel Research, 66(8), pp. 1088–1095, 2010. https://doi.org/10.1016/j.jcsr.2010.03.010

[6] Ahmadie Amiri, H., Najafabadi, E. P., Estekanchi, H. E. "Experimental and analytical study of Block Slit Damper", Journal of Constructional Steel Research, 141, pp. 167–178, 2018. https://doi.org/10.1016/j.jcsr.2017.11.006

[7] Chaboche, J. L. "Time-independent constitutive theories for cyclic plasticity", International Journal of Plasticity, 2, pp. 149–188, 1986. https://doi.org/10.1016/0749-6419(86)90010-0

[8] Xu, L.-Y., Nie, X., Fan, J.-S. "Cyclic behaviour of low-yield-point steel shear panel dampers", Engineering Structures, 126, pp. 391–404, 2016. https://doi.org/10.1016/j.engstruct.2016.08.002

[9] Cheraghi, K. "رگاریم اب ینتب باق ی ا مزرل درکلمع یسررب یکاکطصا" (Evaluation of seismic function of concrete frame with friction damper), MSc Thesis, Razi University, 2017. (in Persian)

[10] Rai, D. C., Annam, P. K., Pradhan, T. "Seismic testing of steel braced frames with aluminum shear yielding dampers", Engineering Structures, 46, pp. 737–747, 2013. https://doi.org/10.1016/j.engstruct.2012.08.027

[11] Hashemi, A., Clifton, G. C., Bagheri, H., Zarnani, P., Quenneville, P. "Proposed design procedure for steel self-centring tension-only braces with resilient connections", Structures, 25, pp. 147–156, 2020. https://doi.org/10.1016/j.istruc.2020.02.024

[12] Mualla, I. H., Belev, B. "Performance of steel frames with a new friction damper device under earthquake excitation", Engineering Structures, 24(3), pp. 365–371, 2002. https://doi.org/10.1016/S0141-0296(01)00102-X

[13] Yousef-beik, S. M. M., Veismoradi, S., Zarnani, P., Quenneville, P. "A new self-centering brace with zero secondary stiffness using elastic buckling", Journal of Constructional Steel Research, 169, 106035, 2020. https://doi.org/10.1016/j.jcsr.2020.106035

[14] Guo, A. X., Xu, Y. L., Wu, B. "Seismic reliability analysis of hysteretic structure with viscoelastic dampers", Engineering Structures, 24(3), pp. 373–383, 2002. https://doi.org/10.1016/S0141-0296(01)00103-1

[15] Ebadi Jamkhaneh, M., Ebrahimi, A. H., Shokri Amiri, M. "Experimental and Numerical Investigation of Steel Moment Resisting Frame with U-Shaped Metallic Yielding Damper", International Journal of Steel Structures, 19(3), pp. 806–818, 2019. https://doi.org/10.1007/s13296-018-0166-z

[16] TahamouliRoudsari, M., Cheraghi, K., Habibi, M. R. "Investigation of retrofitting RC moment resisting frames with ADAS yielding dampers", Asian Journal of Civil Engineering, 20(1), pp. 125–133, 2019. https://doi.org/10.1007/s42107-018-0092-6

[17] TahamouliRoudsari, M., Eslamimanesh, M. B., Entezari, A. R., Noori, O., Torkaman, M. "Experimental Assessment of Retrofitting RC Moment Resisting Frames with ADAS and TADAS Yielding Dampers", Structures, 14, pp. 75–87, 2018. https://doi.org/10.1016/j.istruc.2018.02.005

[18] Aghlara, R., Tahir, M. Md. "A passive metallic damper with replaceable steel bar components for earthquake protection of structures", Engineering Structures, 159, pp. 185–197, 2018. https://doi.org/10.1016/j.engstruct.2017.12.049

[19] Aghlara, R., Tahir, M. M., Adnan, A. B. "Experimental study of Pipe-Fuse Damper for passive energy dissipation in structures", Journal of Constructional Steel Research, 148, pp. 351–360, 2018. https://doi.org/10.1016/j.jcsr.2018.06.004

[20] Yao, Z., Wang, W., Zhu, Y. "Experimental evaluation and numerical simulation of low-yield-point steel shear panel dampers", Engineering Structures, 245, 112860, 2021. https://doi.org/10.1016/j.engstruct.2021.112860

[21] Keyvani Borujeni, A., Mahdi, T. "Reducing the in-plane effect of infill on steel moment frame", International Journal of Steel Structures, 17(3), pp. 1171–1181, 2017. https://doi.org/10.1007/s13296-017-9024-7

[22] Raghu Kumar, B. "Strength of Materials", 1st ed., CRC Press, 2022. ISBN: 9781003298748 https://doi.org/10.1201/9781003298748

[23] AISC "ANSI/AISC 360-16: Specification for Structural Steel Buildings", American Institute of Steel Construction, Chicago, IL, USA, 2016.

[24] Hibbitt, K., Sorensen, I. "ABAQUS/Standard user's Manual Volumes I-III and ABAQUS CAE Manual", Version 6.14, Hibbitt, Karlsson & Sorensen, 2014.

[25] De Matteis, G., Formisano, A., Panico, S., Mazzolani, F. M. "Numerical and experimental analysis of pure aluminium shear panels with welded stiffeners", Computers & Structures, 86(6), pp. 545–555, 2008. https://doi.org/10.1016/j.compstruc.2007.05.027

[26] Guo, L., Rong, Q., Ma, X., Zhang, S. "Behavior of steel plate shear wall connected to frame beams only", International Journal of Steel Structures, 11(4), pp. 467–479, 2011. https://doi.org/10.1007/s13296-011-4006-7

[27] FEMA "FEMA-440 Improvement of Nonlinear Static Seismic Analysis Procedures", Applied Technology Council (ATC-55 Project), Redwood City, CA, USA, 2005.